A15 SURFACES IN Nb CAVITIES

G. Arnolds-Mayer(*)
Wuppertal University, Wuppertal, Germany

1. INTRODUCTION

In the last few years considerable progress was made towards superconducting cavities as accelerating facilities for large e^+e^- storage rings and linear accelerators for nuclear physics research. Recently cavities built from high purity Niobium with improved thermal conductivity have reached accelerating fields of 10 to 15 MV/m. At field levels greater than 5 MV/m the power consumption determined by the cavities Q becomes of major concern. Today cryostat losses are about 5 W/m and the rf losses in the superconducting structures should be of the same value. For Nb cavities this requires an operating temperature below 4.2 K, even at 350 MHz. Cavities made from high T_c materials may have higher Q values resulting in reduced losses and power consumption at 4.2 K.

2. POWER CONSUMPTION IN NIOBIUM CAVITIES

The power P needed to obtain a certain accelerating field E_{acc} is calculated from the relation

$$E_{acc} = \sqrt{(r/Q) \cdot Q_o \cdot P}. \qquad (1)$$

(*) presently at CERN, Geneva

with:

r/Q = shunt impedance

$Q_o = G/R_s$

Q_o = quality factor

G = geometry factor

R_s = surface resistance

From the BCS theory the surface resistance is given by

$$R_s(T) = R_s^{BCS}(T) + R_{res} \quad \text{for } T \leq T_c/2 \qquad (2)$$

$$= A\,\omega^2\, e^{-\Delta_o \frac{T_c}{T}} + R_{res}$$

with $R_s^{BCS}(T)$ = temperature dependent theoretical surface resistance

R_{res} = temperature independent residual resistance

A = material dependent constant

ω = frequency

Δ_o = reduced superconducting energy gap (in units of $k_B T_C$).

Fig. 1 shows the $R_s^{BCS}(T)$ and the temperature dependent Q of niobium cavities at 350 MHz, 1 GHz, and 3 GHz, and gives the temperatures at which a certain field with a given power is obtained. Even for the 350 MHz structures with negligible residual resistance a temperature below 4.2 K is needed to produce a field of 5 MV/m with 5 W per meter of structure. At higher fields, higher Q values are even more important to reduce the power consumption.

3. SURVEY OF HIGH T_c SUPERCONDUCTORS AND THEIR APPLICATION TO RF SUPERCONDUCTIVITY

From eq. (2) one sees that the BCS surface resistance is dominated by the critical temperature T_c. Table 1 lists the binary superconducting materials with critical temperatures higher than 9.2 K, gives some of their superconducting properties, and the fields at which they are studied for or commercially available.

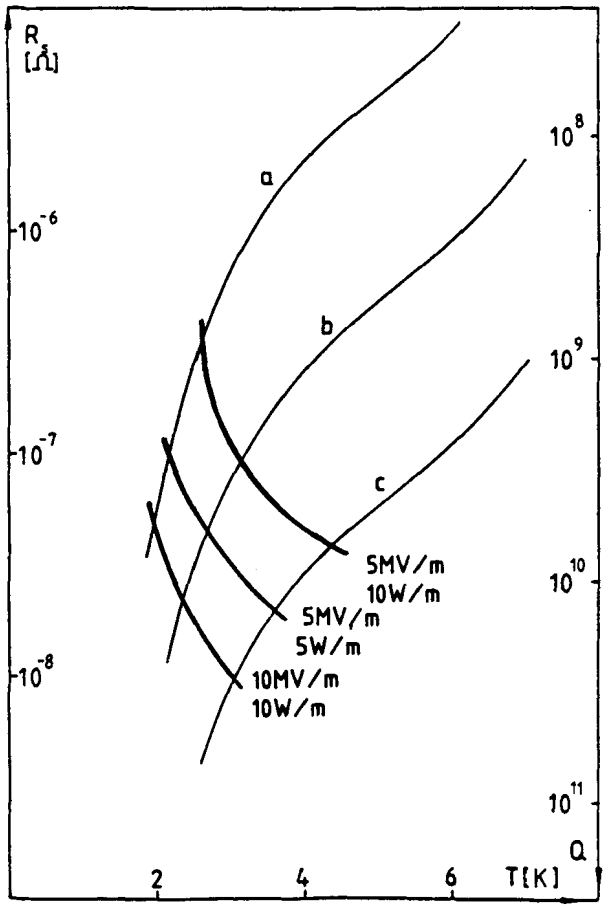

Fig. 1 Temperature dependent surface resistances and power consumption of Niobium cavities (a) frequency 3 GHz, r/Q = 2000 Ω/m (b) frequency 1 GHz, r/Q = 800 Ω/m, (c) frequency 350 MHz, r/Q = 360 Ω/m.

From the phase diagrams (fig. 2) it can be seen that among the interesting A15, high T_c compounds only Nb_3Sn, V_3Ga and V_3Si are easy to produce especially on complex cavities surfaces. The other compounds show extreme narrow stability regions of the A15 phase in the case of vanadium. In the case of Nb based systems the high critical temperatures are obtained only after heat treatments above 1500°C, if not produced by codeposition.

"A 15" describes the crystal structure (fig. 3) of an A_3B compound with Nb or V as A element and B elements from the groups 3 to 5 with filled d shells for the most important high T_c and H_{c2} superconductors. The orthogonal A element chains on the body centered B structure seem to be essential for the high transition temperatures (13).

TABLE 1

Characteristic parameters of binary high T_c superconductors
(exp: experiments, com: commercial available)
(Ref: (1) if not otherwise indicated, (*) see table 2).

Material	Crystal structure	T_c (K)	Δ_o ($k_B T_c$)	$H_{c2}(0)$ (kG)	$H_c(0)$ (kG)	Studied for		
						wires (9)	squids (2)	rf (*)
Nb	bcc	9.2	1.9 (2)	3.8	1.9		com	com
Nb_3Al	A15	18.8	2.15 (2)	295 (5)	6.5		exp	
Nb_3Au	A15	11.5						
NbC	B1	10		19.6	1.2			
Nb_3Ga	A15	20.3		335 (5)		exp		
Nb_3Ge	A15	23.6	2.1 (3)	370 (5)		exp	exp	
NbN	B1	16.1	1.74 (2)	153 (5)	2.2 (6)	exp	exp	exp
Nb_3Pt	A15	10.5						
Nb_3Sn	A15	18.3	2.25 (4)	225	5.3 (7)	com	exp	exp
$NbTc_3$	A12	10.5						
NbTi	bcc	9.8	1.9 (2)	148	2.4 (8)	com	exp	exp
V_3Ga	A15	15.0		350	7.4	com		
V_3Si	A15	17.1	1.78 (2)	156	6.0	exp	exp	exp
Mo_2C	orthoromb.	~ 13		98.5	1.8			
MoN	hexagonal	12	1.8 (2)					
$Mo_{.57}Re_{.43}$		14	1.8 (2)	28	1.6		exp	exp
MoTc		15.8		75			exp	

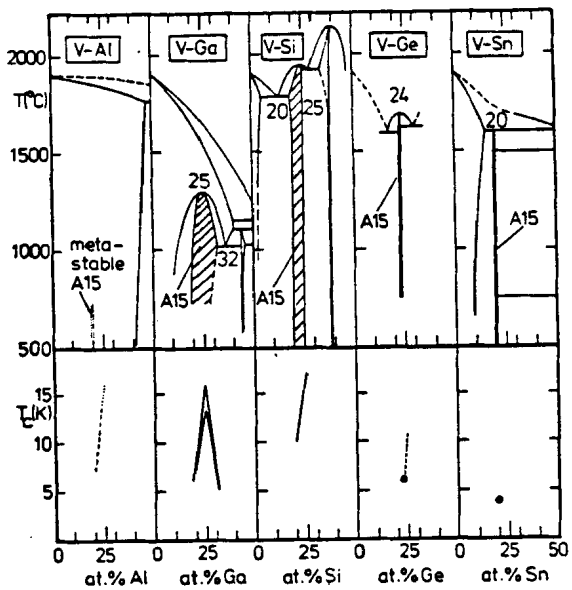

a)

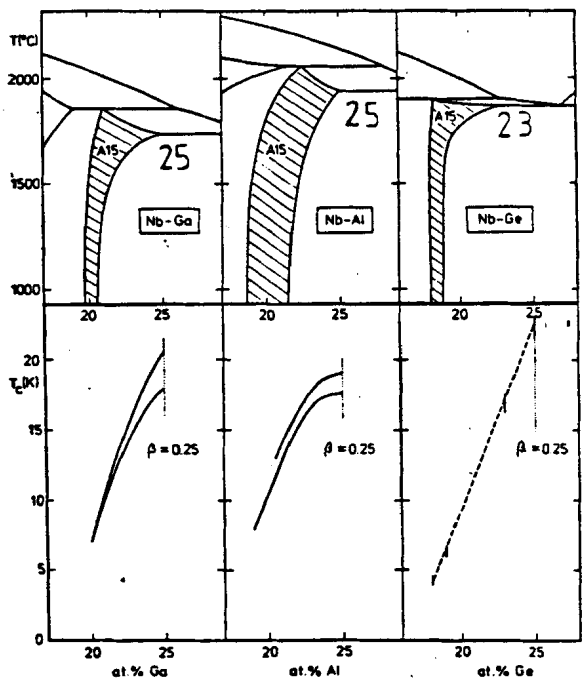

b)

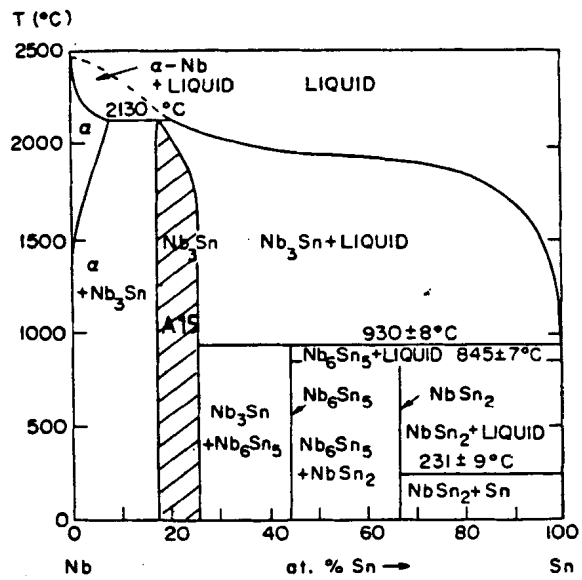

c)

Fig. 2 **Phase fields and critical temperatures of V and Nb based A15 compounds (a, b from (10), c from (11)).**

High T_c superconductors which were studied as cavities materials are: NbTi, MoRe, V_3Si, NbN, and Nb_3Sn. The experimental conditions, preparation methods, and results are listed in table 2. In the case of NbTi (50 : 50 wt %) and MoRe (75 : 25 at %) the cavities were machined from bulk material. The other superconductors were studied as thin films of some microns thickness on niobium or sapphire substrates.

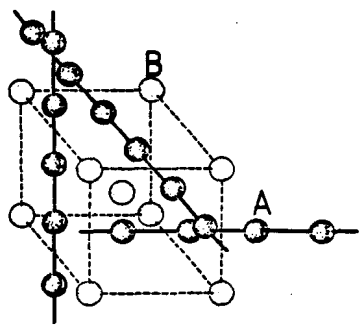

Fig. 3 A15 crystal structure, showing chains of transition metal atoms (from (12)).

For application to accelerating structures the niobium based compounds are of major importance. As large superconducting accelerating units will probably be built out of niobium, it will be less expensive to take those and cover them with a high T_c material instead of making completely new structures.

In the case of the NbN there was up to now no progress compared to Nb cavities, neither in fields nor in the surface resistances. Because of the small energy gap found by rf measurement the theoretical surface resistance at 4.2 K did not exceed the BCS surface resistance of Niobium structures. Probably "wrong" phases which may easily grow, as indicated by the phase diagram (fig. 4), are due to the low value of Δ_o/k_BT_c (16).

As Nb_3Sn seems to be the most advantageous material, preparation methods and rf results will be discussed in the following in detail only for this material.

TABLE 2

High T_c superconductors studied under rf conditions
(ebc: e^- beam co-evaporation, dtv: diffusion from tin vapour
ipt: diffusion from ion plated tin layer, et: diffusion from
evaporated tin layer)

Material	Frequency (GHz)	Resonator type	T_c (K)	$2\Delta_o$ (k_BT_c)	R_s(4.2K) (Ω)	R_{res} (Ω)	H_{peak} (mT)	preparation method	lit
NbTi	9.7	TE011	8.8	3.94	$5,5.10^{-5}$	6.10^{-6}	-	commercial available	(14)
$Mo_{.75}Re_{.25}$	11.3	TE011	10.1	3.56	$1,5.10^{-5}$	$5,7.10^{-7}$	17,6	commercial available	(15)
NbN	6.5	TE011	16.5	2.0	2.10^{-5}	$4,4.10^{-6}$	11,5	reactively sputtered	(16)
V_3Si	8.6	TE011	16.0	-	2.10^{-3}	3.10^{-4}	-	ebc 680°C	(17)
Nb_3Sn	0.1-2	helix		-	-	$1,5.10^{-9}$	83	dtv at 1050°C	(18)
	2.8	TM010	18.1	4.5	$4,5.10^{-7}$	1.10^{-7}	35	dtv at 1050°C & 1500°C	
	2.9	TM010	17.7	4.3	9.10^{-8}	$5,6.10^{-8}$	30	dtv at 1160°C	(19)
	7.6	3 cell acc	17.9	4.3	$3,5.10^{-7}$	$2,2.10^{-7}$	45	dtv at 1130°C	(20)
	8.6	muffin tin	17.7		1.10^{-6}	$8,6.10^{-7}$	38	dtv at 1050°C	(21)
		TM010	17.5		$1,9.10^{-6}$	1.10^{-6}	24	ipt (7μ), 1050°C	
	8.6	TE011	18.0		3.10^{-5}	$1,5.10^{-6}$		ebc 680°C	(17)
	9.6	TE011	18.2		3.10^{-4}	3.10^{-4}		et 880°C	(22)
	9.5	TE011 (Nb rod)			$2.9.10^{-7}$	$1,3\text{-}10^{-7}$	106	dtv at 1050°C	(23)
	10.0	TM010 (Nb sheet)			$3,9.10^{-7}$	$1,5.10^{-7}$	65	dtv at 1050°C	(24)
	20.2	TE113			$1,7.10^{6}$	$1,2.10^{-7}$		dtv at 1230°C	(25)

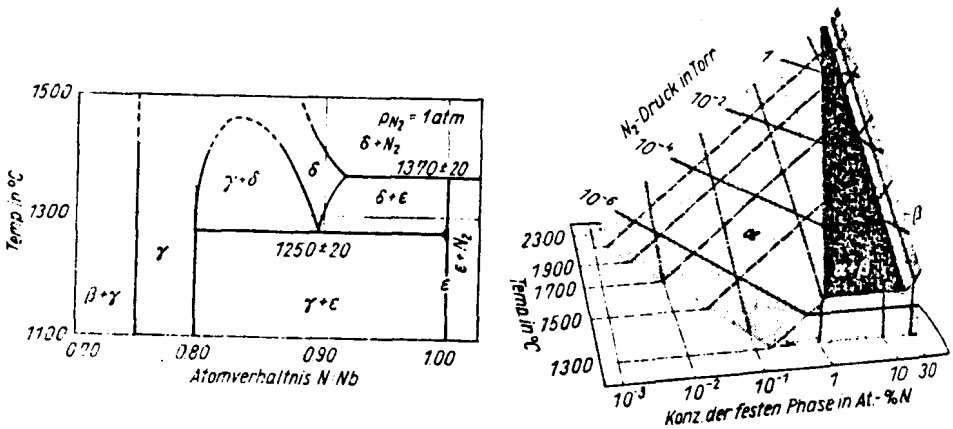

Fig. 4 Phase diagram of the NbN system (from (26)) T_c of δ phase = 16.2 K

4. PREPARATION METHODS OF Nb_3Sn

Up to now the following preparation methods were studied to grow Nb_3Sn on cavities surfaces or parts of those: electron beam co-evaporation (17), diffusion from tin layers (22), (21) and diffusion from tin vapour (18)-(21), (23)-(25).

The electron beam co-evaporation is a very sophisticated procedure, generally used for the production of Josephson junctions. The experimental set up is shown in fig. 5. Critical parameters in making high quality films are the stability and uniformity of the substrate temperature, the configuration and type of the evaporation sources, and the evaporation of the compounds which have to be individually controlled (27). All this makes it very difficult to use e^- beam co-evaporation to cover complex accelerating structures with Nb_3Sn.

To grow Nb_3Sn from tin layers the tin layers were produced by evaporation or ion plating. They have to be homogeneous and of certain thickness, relying on the reaction temperature. If the tin layer is too thin, the resulting Nb_3Sn will be thinner than the penetration depth and the procedure has to be repeated several times (22). If the tin layer is too thick, tin agglomerates during the heat treatment to droplets probably due to the surface tension of the molten tin. These stay

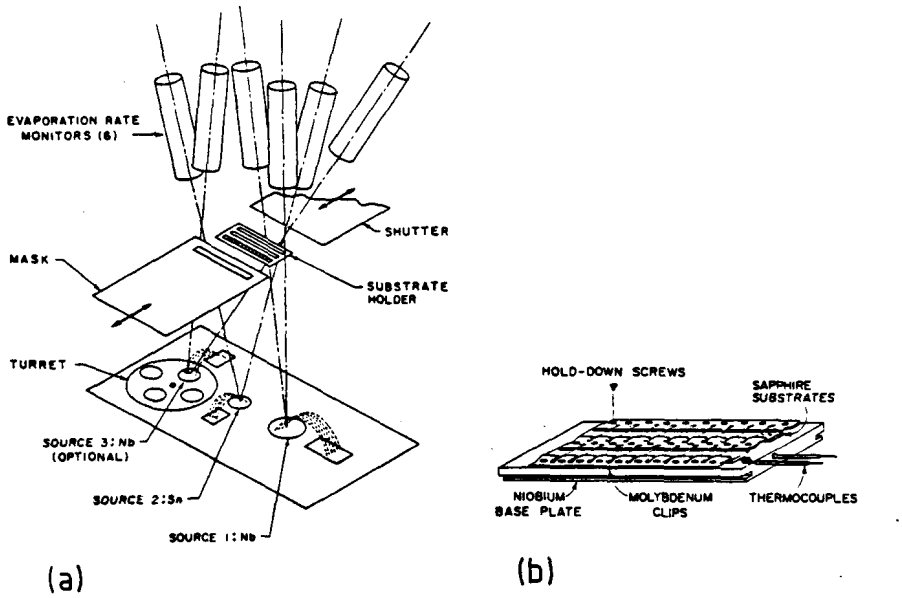

Fig. 5 (a) schematic of electron-beam deposition system showing linear source arrangement; (b) Sample holder design to better control and stabilize substrate temperature during deposition. Niobium baseplate is heated by radiation from behind (from (27)).

unreacted or build up the poor superconducting phases Nb_2Sn_5 or $NbSn_2$ during cool down and lead to enhanced surface resistances (21), (22). To overcome the agglomeration of the tin an additional sputtered Nb layer was experienced leading to reasonable results (21). This technique may also be applied to produce Nb_3Sn on Cu cavities. It would be comparable to the "bronze process" well known from the production of Nb_3Sn wires (as a survey article see (28)). The advantage of a Cu-Nb_3Sn cavity would be the possibly higher Q at 4.2 K, not being as sensitive to thermal oscillations of the bath compared to pure Nb, and the thermal stabilisation of "bad spots" via the high thermal conductivity of the copper.

The most experienced method to get Nb_3Sn covers on Nb cavities is the diffusion from the tin vapour. To produce high quality, homogeneous Nb_3Sn layers the following steps are done:

(1) optimisation of the Nb surface;

(2) anodisation (30 V with NH_3 solution (23), 30 V with HNO_3 solution (19));

(3) prenucleation via tin halogenides ($SnCl_2$, SnF_2 at ~ 500°C under UHV conditions (23));

(4) diffusion from tin vapour (T > 930°C under UHV conditions) (30);

(5) annealing (18) (19);

(6) oxipolishing.

Of course before depositing the Nb_3Sn, the Nb surfaces are optimised by usual treatments. Anodisation and prenucleation were introduced to get cristallisation nuclei on every crystal face of the niobium and to produce a homogeneous layer. But in recent experiments it turned out that neither tin halogenides (24) nor anodisation (31) is essential.

The diffusion process is done at temperatures higher than 930°C to prevent the growing of the phases Nb_2Sn and Nb_6Sn_5.

During the diffusion process a homogeneous temperature distribution is extremely important. Already a temperature degradation of 15°C at some parts of the cavity leads to a severe condensation of tin, which remains partly unreacted on the surface (32). Difficulties concerning crystallisation nuclei were mostly observed after covering cavities made from sheet material. These have thinner walls (typically 1-2 mm) compared to cavities machined from rod material (typically 3-4 mm). It may be that the temperature distribution of the thin walled cavities is less homogeneous compared to the thick walled cavities, resulting in unhomogenous Nb_3Sn layers (29).

The second important parameter during the diffusion process is the tin vapour pressure. It influences mostly the rate of the growth and can be varied by baffles (20) (21), separated heating of tin source and cavity, (18)(19) or displacement of the tin source (24).

The thickness x of a Nb_3Sn diffusion layer with time t corresponds to

$$x \propto t^{\alpha}$$

with $\alpha = 0.36$ (32) (33). Annealing subsequent to the vapour diffusion process is assumed to reduce the unreacted tin on the surface. This would also help to prevent the forming of the phases $NbSn_2$ and Nb_6Sn_5 during cool down. By oxipolishing in NH_3 (24), HNO_3 (32) or NH_4OH (21) solution unreacted tin is continuously dissolved and $NbSn_2$ and Nb_6Sn_5 can be removed. After oxipolishing with NH_3 solutions etching pits were observed on the Nb_3Sn crystallites (29). This was not the case using HNO_3 solutions.

Thermally separated tin source and cavity are advantageous to avoid demounting and remounting the cavity between the heat treatments. Fig. 6 shows the Wuppertal furnace built for 3 GHz structures of a maximum length of 60 cm. The heater of this furnace is made from a molybdenum mesh to get a homogeneous temperature distribution all over the cavity. During annealing at 1150°C the temperature difference between the cavity and the unheated tin source is ~ 500°C. First experiments with this system were performed to study the layer thickness along a 5 cell structure.

After a 20h process at 1160°C a Nb_3Sn layer of (3.5 ± 0.2) µm in cell 1 and (2.1 ± 0.2) µm in cell 5 was measured. This reduction is due to the tin pressure gradient along the cavity and was partly overcome by turning the structure upside down and repeating the diffusion process. After this the layer thickness was (4.4 ± 0.2) µm in cell 1 and (3.3 ± 0.2) µm in cell 5 (31). Adjusted diffusion times before and after turning the cavity will lead to a layer thickness equal in all cells.

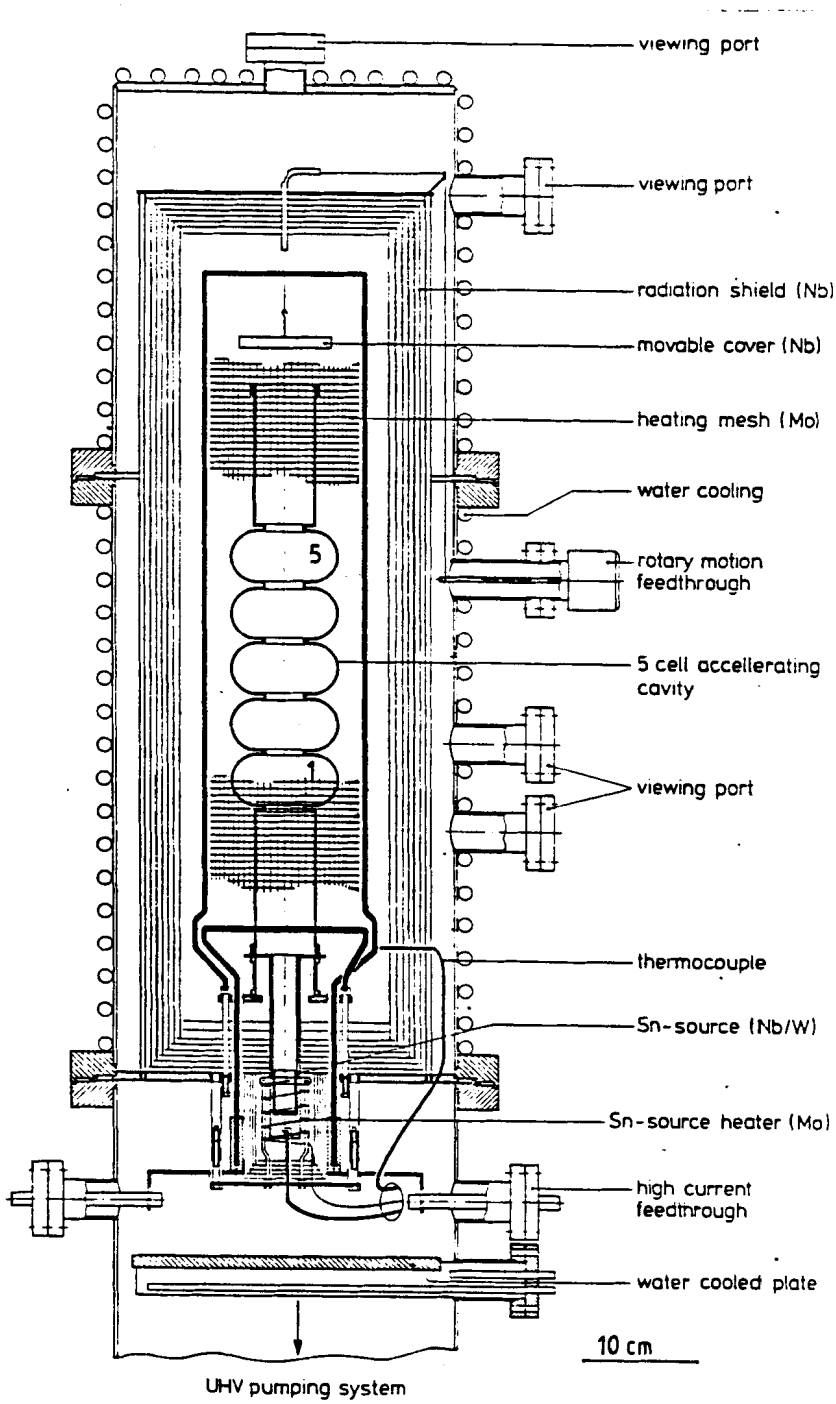

Fig. 6 **UHV furnace to produce Nb_3Sn layers.**

5. RESULTS OF rf EXPERIMENTS

Nb_3Sn can only be a competitive cavities material if the surface resistances at 4.2 K are lower and the accelerating fields are of the same order compared to those reached in Niobium structures.

5.1 Surface resistances

Surface resistances at 4.2 K and residual resistances of Nb_3Sn cavities in the frequency range from 100 MHz up to 20 GHz are displayed in fig. 7. The lines indicate the 4.2 K BCS resistances for Niobium respectively Nb_3Sn. Below ~ 10 GHz both are assumed to scale with ω^2 (34). Comparing the 4.2 K surface resistances of Nb- and Nb_3Sn- cavities a reduction of about 40 was reached at higher frequencies. A reduction of 140 will be the theoretical limit.

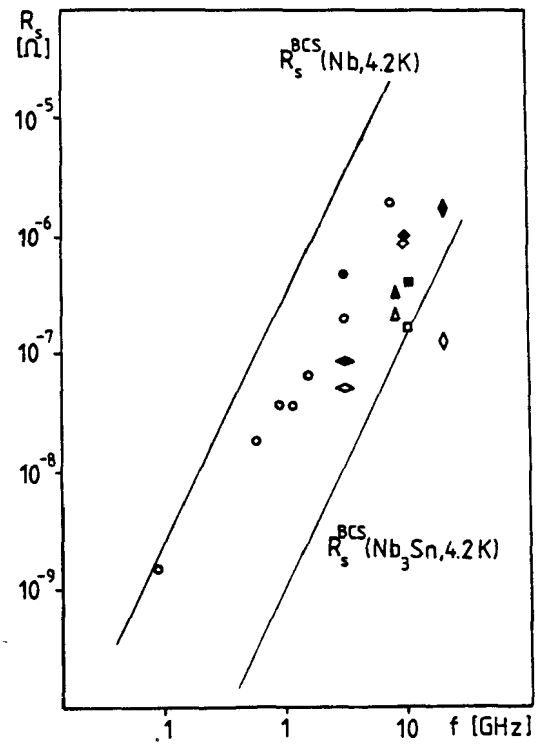

Fig. 7 R_s(4.2 K) and R_{res} from Nb_3Sn (closed symbols R_s(4.2 K), open symbols R_{res}).

(18) (19) (20) (21) (23) (25)

Fig. 8 shows the temperature dependent surface resistances of a 3 GHz Nb_3Sn cavity. The reduction of $R_s(T)$ from Test 3 to Test 5 is due to oxipolishing. The measurements of Test 7 and Test 8 were done after no further treatment of the surface but after a very slow cool down from 77 K to liquid helium temperature.

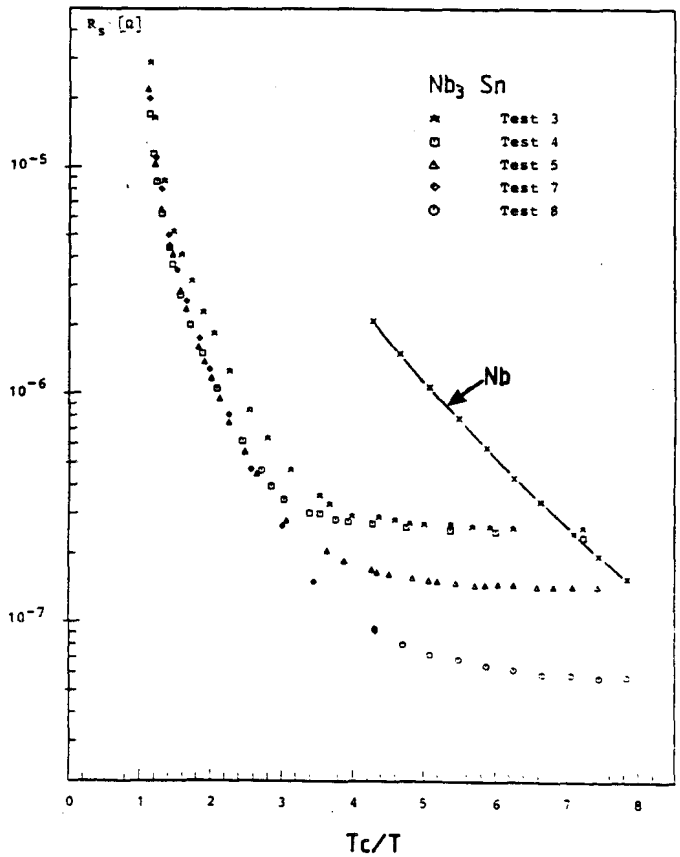

Fig. 8 Temperature dependent surface resistance of a 3 GHz Nb_3Sn cavity (from (19)).

To verify the influence of temperature degradation to the surface resistance the same test was repeated with another Nb_3Sn cavity. During these measurements temperature mapping was applied. The results are shown in fig. 9. The temperature maps were taken in subcooled helium at 2.2 K. The field was 4.6 MV/m in both cases. The temperature structure is the same, showing a place of enhanced powerloss at the same site. But in the case of the slow cool down the overall ΔT level is reduced by about 70 mK corresponding to a Q of $2{,}8.10^9$ instead of $1{,}3.10^9$ after fast cool down. A similar phenomenon was observed on lead plated copper cavities. Frozen flux induced by thermo currents may explain this (35).

experimental set up

resistors

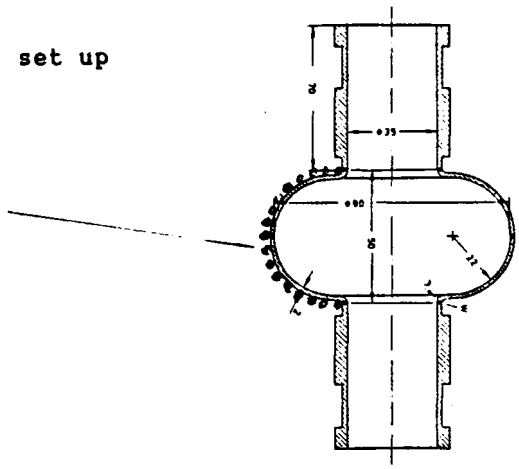

during temperature mapping: subcooled Helium (T = 2.2 K) 4.6 MV/m, 5° steps

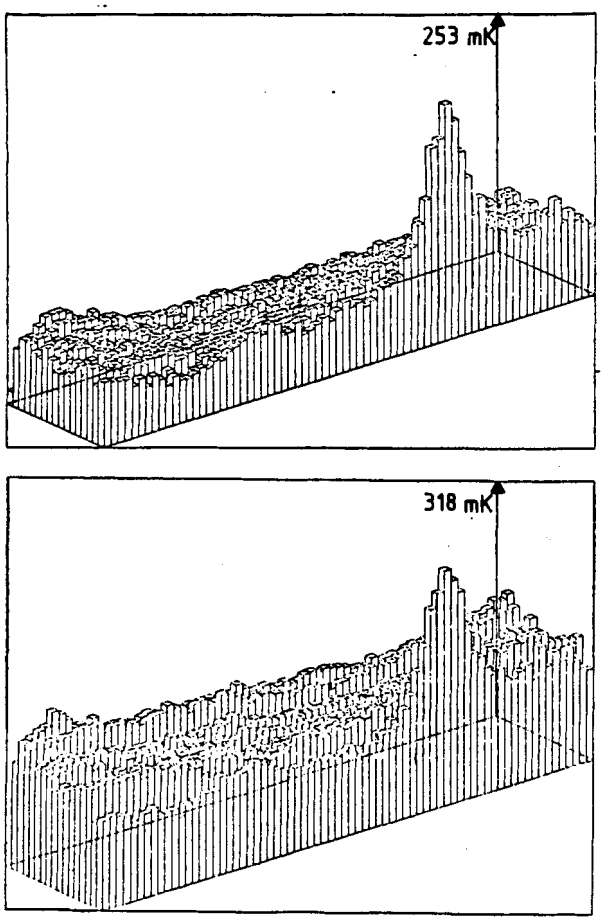

cooling
slow fast
30 K → 16 K → 4.2 K

ΔT_{max} = 253 mK
at Res.1 at 255°

ΔT_{mean} ~ 80 mK
Q = 2.8.10⁹.

Cooling

fast
30 K → 4.2 K

ΔT_{max} = 318 mK
at Res 1 at 255°

ΔT_{mean} ~ 150 mK
Q = 1.3.10⁹

Fig. 9 Temperature map of a 3 GHz Nb_3Sn cavity (31)

5.2 Nb_3Sn cavities under high field operation

The second important feature for the application of Nb_3Sn are the fields which can be reached. Fig. 10 shows the magnetic and electric fields measured with Nb_3Sn cavities at frequencies from 100 MHz to 10 GHz. The fields are comparable to those achieved with cavities made from bad thermal conductivity niobium. The proportionality of E_{peak} and H_{peak} to the frequency seems to represent the probability of producing defects on the surfaces. Fig. 11 shows the Q dependent on the accelerating field measured with the 3 GHz cavity after slow and fast cool down (a, a') and a 10 GHz cavity (b). In all cases the fields are limited by quenching and a reduction of Q of about 2-3 is observed. In the case of the 3 GHz structure this degradation is obviously induced by electron currents.

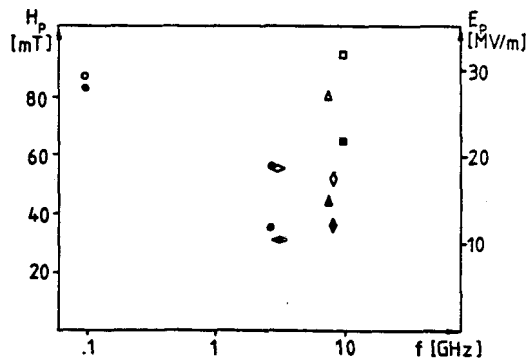

Fig. 10 Magnetic and electric peak fields (closed symbols: H_p, open symbols E_p) ○● (18)◇◆(19)△▲ (20) ◊ ♦ (21) □■ (23)

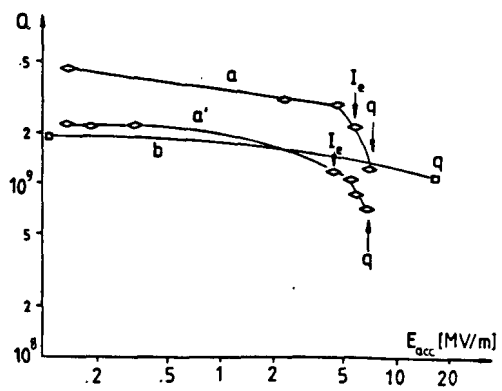

Fig. 11 Field dependent quality factor of Nb_3Sn cavities (a, a': (31); b: (23)).

6. DC FIELD EMISSION AND SECONDARY ELECTRON EMISSION COEFFICIENTS FROM Nb_3Sn SURFACES

As field emission and multipacting limit the accelerating fields of superconducting cavities the characteristics of Nb_3Sn in this respect have to be comparable to those of Niobium.

Fig. 12 shows the results of dc field emission measurements of Nb (36) and Nb_3Sn (37) done with plane-to-plane geometry on anodized and non anodized surfaces.

Before the measurements a surface layer of 2nm was removed by argon glow discharge in the case of Nb_3Sn while the Nb samples were baked for about 30-40 hours at around 200 to 250°C. In fig. 12 (a) field

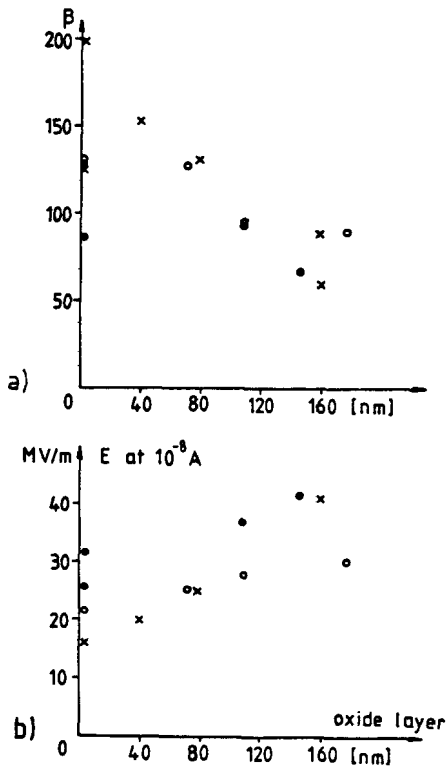

Fig. 12 Results of electron field emission measurements of Nb and Nb_3Sn and their anodic oxides. (a) field enhancement factor β; (b) voltage at a current of 10^{-8} A; (x: Nb from (36); o: 2 μm Nb_3Sn; •: 0.5 μm Nb_3Sn from (37)).

enhancement factors β calculated from the Fowler-Nordheim equation are plotted against the oxide layer thickness. For both materials, the field enhancement factors are very similar and go down with increasing oxide layer thickness. Fig. 12(b) shows the fields at which a current of 10^{-8} A was measured. At higher currents many times instabilities produced by activation or inactivation of electron emitters and electrical breakdowns were observed. The fields at the current of 10^{-8} A increase with the thickness of the oxide layer in both cases without significant differences. But it seems that very thin Nb_3Sn layers are emitting less electrons than thicker ones.

Care must be taken to avoid electrical breakdowns during the measurements. They lead to a severe destruction of the Nb_3Sn surface (fig. 13) with tin evaporation and enhanced electron emission.

Secondary electron emission coefficients δ of methanol rinsed Nb_3Sn samples (fig. 14(c)) are very similar to δ's measured on Nb samples at CERN (38) but higher than those found at Cornell (39) on wet treated samples (fig. 14(a)). After removing a surface layer of 400 Å (Nb) respectively 20 Å (Nb_3Sn) of the non anodized samples, δ_{max} is reduced to 1.25 ± 0.1. Comparable values are measured on anodized Nb samples before and after cleaning the surface (fig. 14(a) and 14 (c)). On both materials the oxide layers reduce significantly the energy range of the incident electrons at which δ is higher than 1.

The Auger spectra show similar oxygen affinity of Nb and Nb_3Sn under clean conditions and the change of the carbon peak into a carbide peak after sputtering (fig. 14(b) and 14(d)). Measurements on Nb and Nb_3Sn surfaces during electron bombardment resulted in comparable sorption layers, work functions and secondary electron yields on both materials and their oxides (40).

(a)

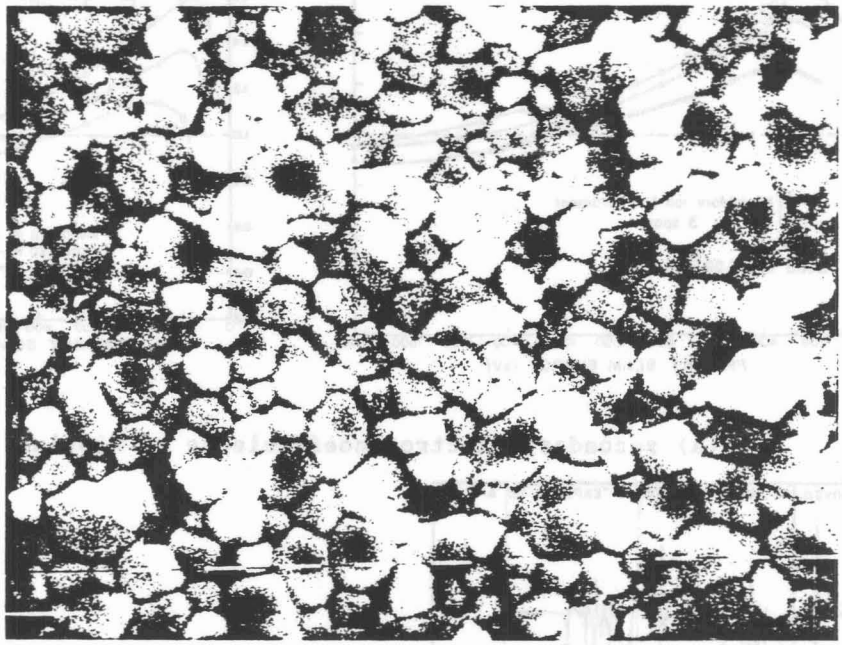

(b)

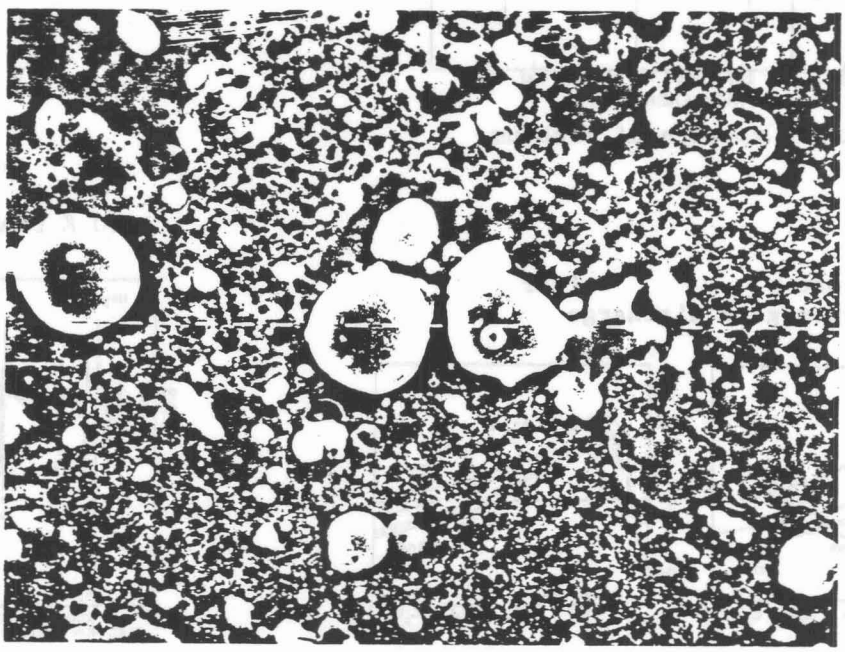

Fig. 13 Nb_3Sn surfaces (white bar = 1 μm)

(a) undisturbed surface
(b) surface destroyed by electrical breakdowns.

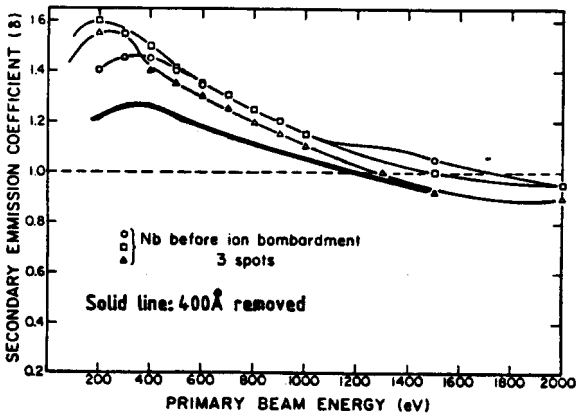

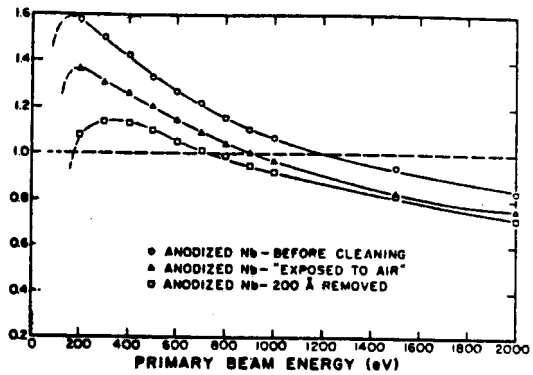

(a) secondary electron coefficients of Niobium

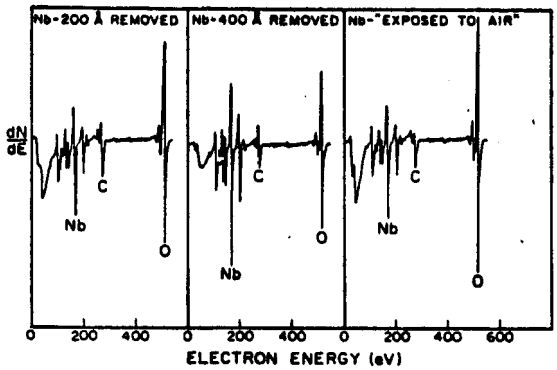

(b) Auger spectra of Niobium

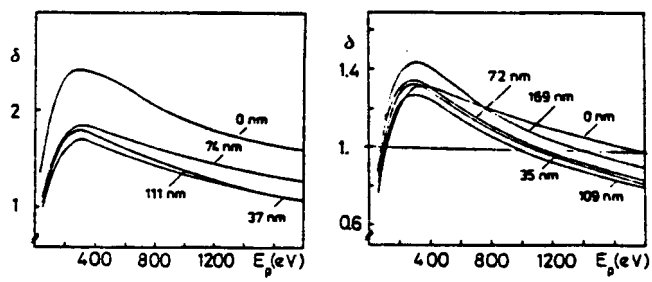

(c) secondary electron yields of Nb_3Sn

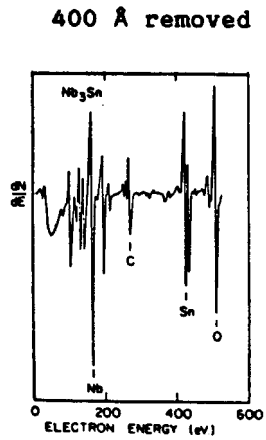

(d) Auger spectrum of Nb_3Sn

Fig. 14: Secondary electron emission coefficients and Auger spectra from Niobium-, and Nb_3Sn surfaces, ((a), (b) and (d) from (39), (c) from (37)).

7. CONCLUSION

Up to now Nb_3Sn is the only high T_c superconductor competitive with Nb in accelerator applications. The existing fabrication methods for thin Nb_3Sn layers have allowed to reach comparable field levels to the ones obtained in Nb cavities and in the frequency range of 3-20 GHz. At 4.2 K the Q_o values reached are 30 to 40 times higher than the theoretical Q values of Niobium. Furthermore there are no significant differences between the two materials with respect to field emission and secondary electron yields. Hence it appears that Nb_3Sn is an extremely interesting alternative to Nb for superconducting acceleration structures.

Further studies should concentrate on the application of Nb_3Sn at frequencies well below 3 GHz. The use of high thermal conductivity Niobium or even copper as a substrate material would be of great interest. Finally an increased back up by modern surface analysis methods will be essential for understanding the limiting effects of surface defects and Nb_3Sn layer inhomogeneities.

REFERENCES

[1] Handbook of Chemistry and Physics CRC Press, Boca Raton Florida 1983.

[2] M.R. Beasley and C.J. Kirchner, Josephson junctions electronics: materials issues and fabrication techniques, from: Superconductor Materials Science, Metallurgy, Fabrication and Applications, Editors S. Foner and B.B. Schwartz, Plenum Press New York (1981).

[3] D.F. Moore, R.B. Zubeck, J.M. Rowell and M.R. Beasley, Phys. Rev. B20 (1979) 2721.

[4] G. Arnolds and D. Proch, IEEE Trans. Magn. MAG-13, (1977) 500.

[5] R. Roberge, Alternative fabrication technologies for A15 multi-filamentary superconductors, from: Superconductor Materials Science, Metallurgy, Fabrication and Applications, Editors S. Foner and B.B. Schwartz, Plenum Press New York (1981).

[6] K. Hechler, G. Horn, G. Otto, E. Saur and J. Low, Temp. Phys. 1 (1969) 29.

[7] L.J. Vieland and A.W. Wicklund, Phys. Rev. 166 (1968) 424.

[8] R.G. Hampshire and M.T. Taylor, J. Phys. F2 (1972) 89.

[9] M.N. Wilson, Practical superconducting materials, from: Superconductor Materials Science, Metallurgy, Fabrication and Applications, Editors S. Foner and B.B. Schwartz, Plenum Press New York (1981).

[10] R. Flükiger, Experimental determination of high temperature phase diagrams, from: Superconductor Materials Science, Metallurgy, Fabrication and Applications, Editors S. Foner and B.B. Schwartz, Plenum Press New York (1981).

[11] J.P. Charlesworth, I. Macphail and P.E. Madsen, J. Mat. Sci. 5 (1970) 580.

[12] J.K. Hulm and B.T. Matthias, Overview of superconducting materials development, from: Superconductor Materials Science, Metallurgy, Fabrication and Applications, Editors S. Foner and B.B. Schwartz, Plenum Press New York (1981).

[13] J. Labbé and J. Friedel, Journ. de Physique. 27 (1966) 153 and 303.

[14] A. Philipp, K. Lüders and K.D. Kramer, Cryogenics (1978) 641.

[15] K. Agyeman, I.M. Puffer, J.A. Yasaitis and R.M. Rose, IEEE Trans. Magn. MAG-13 (1977) 343.

[16] S. Isagawa, Journ. Appl. Phys. 52 (1981) 921.

[17] L.H. Allen, M.R. Beasley, R.H. Hammond and J.P. Turneaure, IEEE Trans. Magn. MAG-19 (1983) 1003.

REFERENCES (Cont'd)

[18] P. Kneisel, O. Stoltz and J. Halbritter, IEEE Trans. Magn. MAG-15 (1979) 21.

[19] M. Peiniger, Diplomarbeit Wuppertal University, WUD 83-1 Wuppertal 1983.

[20] G. Arnolds, R. Blaschke, H. Piel and D. Proch, IEEE Trans. Magn. MAG-15 (1979) 613.

[21] J. Stimmel, Thesis, Cornell University (1978).

[22] J. Hasse, W.D. Hermann and R. Orlich, Zeitsch. für Phys. 271 (1974) 265.

[23] B. Hillenbrand, H. Martens, H. Pfister, K. Schnitzke and Y. Uzel IEEE Trans. Magn. MAG-13 (1977) 491.

[24] N. Krause, B. Hillenbrand, Y. Uzel and K. Schnitzke, Appl. Phys. A30 (1983) 67.

[25] N. Klein (Wuppertal University) private communication (1984).

[26] Gmelin, Handbuch der anorganischen Chemie Springer Verlag Berlin-Heidelberg-New York (1974).

[27] D.A. Rudman, F. Hellman, R.H. Hammond and M.R. Beasley, Journ. Appl. Phys. 55 (1984) 3544.

[28] M. Suenaga, Metallurgy of continuous filamentary A15 superconductors, from: Superconductor Materials Science, Metallurgy, Fabrication and Applications, Editors S. Foner and B.B. Schwartz, Plenum Press New York (1981).

[29] B. Hillenbrand, N. Krause, K. Schnitzke and Y. Uzel, Forschungsbericht NT 2024 7 Siemens AG Erlangen 1982.

[30] E.J. Saur and J.P. Wurm, Naturwissenschaften 49 (1962) 127.

[31] M. Peiniger (Wuppertal University) private communication.

[32] G. Arnolds, Thesis Wuppertal University, WU B 79-14, Wuppertal 1979.

[33] C.F. Old and I. Macphail, Journ. Mat. Sci. 4 (1969) 202.

[34] R. Blaschke, U. Klein, G. Müller, Interner Bericht Wuppertal University WU B 82-20 Wuppertal (1982).

[35] J.M. Pierce, Journ. Appl. Phys. 44 (1973) 1342.

[36] G.J. Sayag, Nguyen Tuong Viet, H. Bergeret and A. Septier Journ. Phys. E10 (1977) 176.

[37] G. Arnolds-Mayer and N. Hilleret, Adv. Cryog. Eng. Mat. 28 (1982) 611.

REFERENCES (Cont'd)

[38] N. Hilleret, CERN private communication (1984).

[39] H. Padamsee and A. Joshi, Journ. Appl. Phys. 50 (1979) 1112.

[40] M. Grundner and J. Halbritter, Journ. Appl. Phys. 51 (1980) 5396.